Biosensors and Bioelectronics 60 (2014) 130–136

Contents lists available at ScienceDirect

Biosensors and Bioelectronics

journal homepage: www.elsevier.com/locate/bios

Orientation of llama antibodies strongly increases sensitivity of biosensors

Anke K. Trilling [a,b], Thamara Hesselink [a], Adèle van Houwelingen [a], Jan H.G. Cordewener [a], Maarten A. Jongsma [a], Sanne Schoffelen [c], Jan C.M. van Hest [c], Han Zuilhof [b,d], Jules Beekwilder [a,*]

[a] Plant Research International, Wageningen, The Netherlands
[b] Laboratory of Organic Chemistry, Wageningen University, Wageningen, The Netherlands
[c] Department of Bioorganic Chemistry, Institute for Molecules and Materials, Radboud University Nijmegen, Nijmegen, The Netherlands
[d] Department of Chemical and Materials Engineering, King Abdulaziz University, Jeddah, Saudi Arabia

ARTICLE INFO

Article history:
Received 16 February 2014
Received in revised form
4 April 2014
Accepted 7 April 2014
Available online 18 April 2014

Keywords:
Surface plasmon resonance
Llama heavy-chain antibodies
Site-specific azide incorporation
Orientation
Foot-and-mouth disease virus

ABSTRACT

Sensitivity of biosensors depends on the orientation of bio-receptors on the sensor surface. The objective of this study was to organize bio-receptors on surfaces in a way that their analyte binding site is exposed to the analyte solution. VHH proteins recognizing foot-and-mouth disease virus (FMDV) were used for making biosensors, and azides were introduced in the VHH to function as bioorthogonal reactive groups. The importance of the orientation of bio-receptors was addressed by comparing sensors with randomly oriented VHH (with multiple exposed azide groups) to sensors with uniformly oriented VHH (with only a single azide group). A surface plasmon resonance (SPR) chip exposing cyclooctyne was reacted to azide functionalized VHH domains, using click chemistry. Comparison between randomly and uniformly oriented bio-receptors showed up to 800-fold increase in biosensor sensitivity. This technique may increase the containment of infectious diseases such as FMDV as its strongly enhanced sensitivity may facilitate early diagnostics.

1. Introduction

Biosensors combine analytical devices with bio-receptors to sense the presence of analytes. Typical bio-receptors are antibody proteins which are widely used in biosensors due to their high specificity. In addition to full-sized antibodies (e.g. Immunglobulin G [IgG]), fragments of antibodies, such as Fabs (fragment, antigen binding) have been employed in biosensors (Chen et al., 2010; Yoshimoto et al., 2010). These fragments contain the analyte recognition site, but can be designed and produced as recombinant proteins for applications in biosensors (Conroy et al., 2009; Zeng et al., 2012). The smallest natural antibody-based binding unit is the variable domain of llama heavy-chain antibodies (VHH), which has a diameter of a few nm (Hamers-Casterman et al., 1993; Deffar et al., 2009). Such binding fragments are attractive for nanotechnology, since they can be easily tailored by protein engineering and included in biosensors (Saerens et al., 2005; Trilling et al., 2011).

Immobilization methods have an impact on the analytical performance in biosensors, as they affect the lifetime and orientation of the antibodies. Amine groups located at the surface of the antibody are often used to attach the protein covalently to activated carboxyl groups on sensor materials (Trilling et al., 2013a; Vashist et al., 2011). This method results in a random orientation, which reduces the efficiency of the sensor, as a large portion of the antibodies will not expose the analyte binding site to the analyte solution. Several techniques to position the antibodies in a uniform orientation on the surface have been explored, such as protein A or G for immunoglobulin or the biotin-streptavidin system (Bereli et al., 2011; Trilling et al., 2013a, 2013b; Huy et al., 2011; Park et al., 2011a, 2011b; Song et al., 2011). A common drawback of these methods is that they require an intermediate protein and rely on non-covalent protein–protein interactions. Inevitably this will negatively affect the lifetime of the biosensor and increase the distance between capture component and sensor surface (Trilling et al., 2013a). To establish stable covalent links to proteins in an aqueous environment, biocompatible click reactions, such as the 1,3-dipolar cycloaddition between an azide and an alkyne, have recently been developed (Kolb et al., 2001). Such reactions can be catalyzed by copper(I), or may occur in the absence of a catalyst, when the ligand contains a highly strained cyclic alkyne (e.g. cyclooctyne) with a low activation energy (so-called copper(I)-catalyzed azide-alkyne cycloaddition [CuAAC] and strain-promoted alkyne-azide cycloadditions [SPAAC] reactions, respectively) (Debets

* Corresponding author.
E-mail address: jules.beekwilder@wur.nl (J. Beekwilder).

http://dx.doi.org/10.1016/j.bios.2014.04.017
0956-5663/

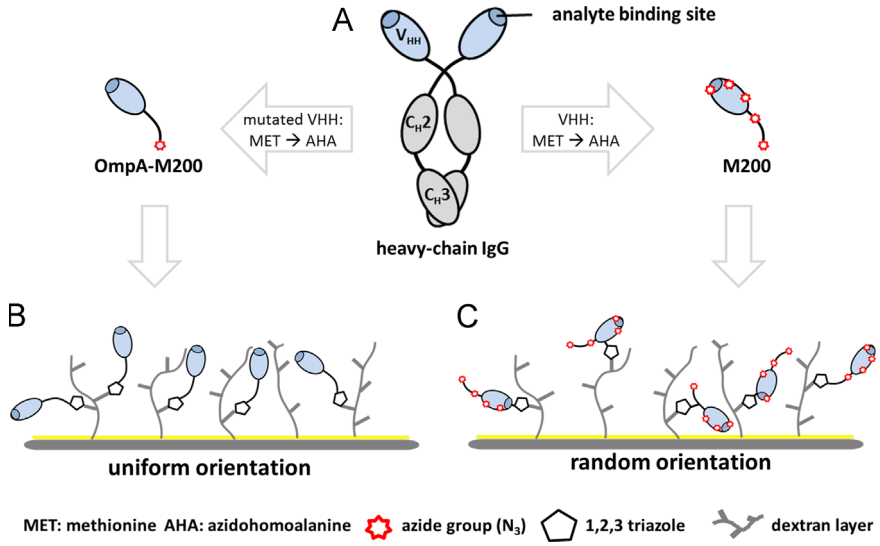

Fig. 1. Schematic illustration of the orientation of immobilized VHHs with tailor-made modifications on a sensor chip. (A) Azide-functionalized VHH receptors M200 and engineered VHH OmpA-M200 are smaller analogues of full llama heavy-chain IgG. (B) Azide-functionalized VHH OmpA-M200 covalently coupled in a uniform orientation onto a cyclooctyne-functionalized CM5 sensor. (C) Azide-functionalized VHH M200 covalently coupled in a random orientation via one of 5 available azides onto a cyclooctyne-tailored CM5 sensor.

et al., 2011; Jewett and Bertozzi, 2010). Azides may be incorporated into proteins as the non-natural amino-acid azidohomoalanine (AHA), an analogue which replaces methionine (Kiick et al., 2002). In this way, click chemistry has been deployed for the labelling of cells by dye conjugation, or for establishing enzyme complexes (Hong et al., 2010; Schoffelen et al., 2010). Here we explore both the CuAAC and SPAAC reactions to finally obtain a uniform orientation of VHH antibodies onto a surface plasmon resonance (SPR) biosensor surface (Fig. 1). This biosensor detects epitopes from foot-and-mouth disease virus (FMDV), and the virus itself.

2. Material and methods

2.1. Variable domain of llama heavy-chain antibodies (VHH)

VHH M200 (GenBank accession no: AJ811563.1) is specific for peptide PAT49 (acetyl-YGDGTVANVRGDLQVLAQKAARALPC-amide), corresponding to amino acid residues 136-160 of the GH-loop of the foot-and-mouth disease virus (FDMV) of the O1 Mansia strain (Harmsen et al., 2007). Native VHH M200-encoding DNA is present in the PRI-VSV expression vector (Trilling et al., 2013a). A variant (OmpA-M200) of this plasmid was made which expresses a protein with only a single methionine. To this end two internal methionine codons (coding for M83 and M88: Fig. 2) were altered to alanines by overlap extension PCR using oligonucleotides M200-M83A-M88A-F and M200-M83A-M88A-R (ESI, Table S1). Subsequently, the methionine residue (M153) in the C-terminal part of the protein, just before the His_6 tag was altered to glycine using the same strategy and oligonucleotides M200-M153G-F and M200-M153G-R. A methionine was introduced at the C-terminus by introducing six additional nucleotides (GGGATG) before the stop codon, encoding glycine and methionine, by amplifying the engineered M200 fragment using oligonucleotides M200-F and M200-R, and recloning the engineered fragment in the PstI/NotI restriction sites of the PRI-VSV expression vector. Lastly, an OmpA signal sequence was introduce at the N-terminus of engineered M200 using oligonucleotides OmpA-F and OmpA-R. Oligonucleotides were hybridized and ligated into PstI/NdeI digested PRI-VSV expression vector. Introduction of OmpA signal sequence results in loss of N-terminal start methionine in the mature protein. The entire VHH fragment of the resulting plasmid PRI-VHH-OmpA-M200 (Fig. 2) was analyzed by DNA sequencing using oligonucleotides M200-F and M200-R.

2.2. Expression and purification of recombinant VHHs

Plasmids PRI-VHH-M200 and PRI-VHH-OmpA-M200 were introduced into *Escherichia coli* B834 (DE3) pLysS bacteria (Novagen). Bacteria were used for protein expression as previous described (Trilling et al., 2011). AHA synthesis and expression of AHA containing VHHs (VHH-AHA) were performed as described before (Schoffelen et al., 2008). To obtain recombinant protein, bacteria were lysed by sonication. In short, pellets were dissolved in 1/10 volume lysis buffer (50 mM NaH_2PO_4, 300 mM NaCl, adjusted to pH 6.0), complemented with 1/100 volume protease inhibitor cocktail (Sigma, St Louis) and 1 mg mL^{-1} lysozyme. Lysozyme digestion was allowed for 30 min at 4 °C before cells were sonicated with a Soniprep150 (MSE, London, United Kingdom) in 5 mL batches for 10 cycles á 10 s with a break of 10 s. Cell lysate was then centrifuged for 30 min at 13.000 rpm and 4 °C. Supernatant was used for VHH purification using Ni-NTA Superflow resin (QIAGEN, Germany) as reported before (van Houwelingen et al., 2008). Eluates were concentrated to 200 μL using Amicon ultra-15 centrifugal filter units (cut-off 10K, Millipore, the Netherlands). Further purification was performed by size exclusion chromatography using a Superdex 200 GL 10/300 column on an ÄKTA FPLC™. VHHs were stored with a final concentration of 15% glycerol at −20 °C. Protein concentration was determined using Bradford test (Bradford, 1976) while successful expression and purification was verified by 15% sodium dodecylsulphate polyacrylamide gel electrophoresis (SDS-PAGE) stained with SYPRO ruby (BioRad, the Netherlands).

2.3. Investigation of engineered VHH by enzyme linked immunosorbent assay (ELISA)

Wells of ELISA plates (Maxisorb, NUNC, the Netherlands) were coated with 5 μg mL^{-1} peptide PAT49 in 50 mM carbonate buffer pH 9.6 and incubated at 4 °C overnight. Antigen-coated wells were emptied and washed three times with 200 μL 10 mM phosphate-buffered saline pH 7.4 (PBS) with 0.05% Tween 20 (PBST) and then blocked with 200 μL PBS containing 3% nonfat powdered milk (w/v)

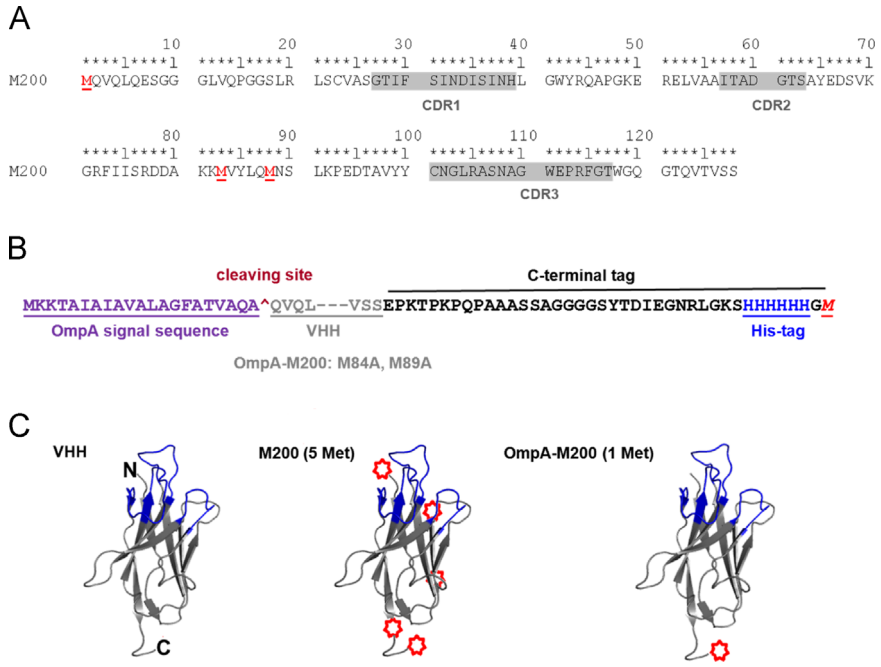

Fig. 2. Structure of VHHs. (A) Protein sequence of VHH M200. The three complementarity determining regions CDR1, CDR2 and CDR3 are shaded; methionine residues are underlined and red. (B) Protein sequence showing engineered VHH OmpA-M200 construct. (C) Crystal structure of llama VHH domain raised against a carbazole hapten (PDB entry 1U0Q) showing N- and C-terminal position in VHH, CDR loops shown in blue (left). Red stars at methionine positions were introduced representative for VHH M200 before (M200, middle) and after engineering (OmpA-M200, right). (For interpretation of the references to color in this figure legend, the reader is referred to the web version of this article.)

and 0.05% Tween 20 (3% PBSMT) for 8 h at room temperature. Wells were emptied and washed three times with 200 μL PBST. 100 μL VHH at indicated concentration in PBS was added and binding was allowed to occur at 4 °C overnight. Excess VHHs were removed by washing three times with 200 μL PBST and 100 μL anti-His_6-PO conjugate (Sigma Aldrich, Missouri, USA) was added at a 1:2000 dilution for 1 h in 3% PBSMT. The anti-His6-PO conjugate is an antibody directed against the His_6 tag conjugated with the enzyme horseradish peroxidase. Excess conjugate was washed off one time with 200 μL PBST and two times with 200 μL demi water. Subsequently peroxidase activity was determined by adding 1-StepTM Ultra 3,3′,5,5′-tetramentylbenzidine (TMB) ELISA substrate (Pierce, Rockford, IL). The reaction was allowed to proceed in the dark for 30 min and then stopped with 50 μL 1 M sulphuric acid. The absorbance was measured at 415 nm in a microtiter plate-reader (TECAN SpectraFluor Microplate Reader). All samples were measured in duplicates.

2.4. Click reaction with VHH

Bicyclo[6.1.0]non-4-yn-9-ol-polyethylene-glycol 5000 (BCN-PEG_{5000}) conjugate was purchased from Synnaffix (Nijmegen, the Netherlands). DIBO-PEG_{2000} was supplied by Marjoke Debets (Nijmegen University, the Netherlands). Alkyne-PEG_{5000} was synthesized as described before (Deiters et al., 2004). Bathophenanthroline sulfonated sodium salt was purchased from GFS Chemicals (Powell, US).

Click reactions were carried out overnight at ambient temperature. The CuAAC was performed in Click solution (1 vol. of 0.1 M CuBr with 2 vol. of 0.1 M ligand [bathophenanthroline sulfonated sodium salt] in DMSO/*t*-BuOH 3:1). 20 μL phosphate buffer containing 2 μL click solution and 2 μg VHH were reacted with 1 mM alkyne-PEG_{5000}. SPAAC was performed in 20 μL phosphate buffer containing 2 μg VHH and 1 mM alkyne-reagent (BCN-PEG_{5000} or DIBO-PEG_{2000}). Reactions were quenched by addition of 5 mM benzyl azide in DMSO. Quenching was allowed for 3 h at ambient temperature before the efficiency of the click reaction was verified by SDS-PAGE protein chromatography.

2.5. Surface plasmon resonance (SPR)

The BIAacore 3000, carboxymethyl dextran sensor chips (CM5), HBS-EP buffer (pH 7.4, consisting of 10 mM 4-(2-hydroxyethyl) piperazine-1-ethanesulfonicacid, 150 mM sodium chloride, 3 mM ethylenediaminetetraacetic acid, 0.005% v/v surfactant polysorbate 20), the amine coupling kit (containing 0.1 M *N*-hydroxysuccinimide (NHS), 0.4 M 1-ethyl-3-(3-dime-thylaminopropyl)carbodiimide hydrochloride (EDC) and 1 M ethanolamine hydrochloride (pH 8.5)) were purchased from GE Healthcare (Uppsala, Sweden). *N*-(1R,8S,9s)-bicyclo[6.1.0]non-4-yn-9-ylmethyloxycarbonyl 1,8-diamino-3,6-dioxaoctane (BCN-POE_3-NH_2) was purchased from Synnaffix (Nijmegen, the Netherlands). The experiment was replicated with two chips, which produced comparable results.

BCN functionalized surface: In a BIAcore 3000 alkyne-functionalized surfaces were prepared using standard EDC/NHS coupling chemistry. To this end the CM5 biosensor surface was activated by injecting a mixture of EDC and NHS (1:1; v/v, 35 μL at a flow rate of 5 μL min^{-1}) into flow channels (Fc1, Fc3 and Fc4). Then 50 μL BCN-POE_3-NH_2 (0.1 mg mL^{-1} in 10 mM maleic acid pH 6.0) was injected and bound to the activated carboxymethylated dextran surface via its primary amine groups. After coupling, the remaining active groups were blocked with ethanolamine hydrochloride (35 μL at a flow rate of 5 μL min^{-1}).

Reference channel (Fc1): All active free cyclooctynes of the BCN functionalized surface were blocked with 35 μL 2-azidoethanol (0.1 mg mL^{-1} in HBS-EP buffer at a flow rate of 5 μL min^{-1}).

Random orientation by NHS chemistry (Fc2): The biosensor surface was activated by injecting (35 μL at a flow rate of 5 μL min^{-1}) a mixture of EDC and NHS (1:1, v/v) into flow channel Fc2. Then M200-AHA VHH (50 μg mL^{-1} diluted in coupling buffer [10 mM sodium acetate, pH 4.0]) was injected and bound to the activated carboxymethylated dextran surface via its primary amine groups, aiming for a similar immobilization level as Fc3. After

coupling, the remaining active groups were blocked with ethanolamine hydrochloride (1 M, 35 μL at a flow rate of 5 μL min^{-1}). Immobilization of M200-AHA on Fc2 resulted in 4809 RU for chip1 and 3103 RU for chip 2.

Random orientation by click chemistry (Fc3): 50 μg mL^{-1} M200-AHA in 10 mM sodium acetate, pH 4.0 was immobilized (120 μL at a flow rate of 5 μL min^{-1}) on the BCN functionalized surface. After VHH coupling, the remaining active free cyclooctynes were blocked with 35 μL 2-azidoethanol (0.1 mg mL^{-1} in HBS-EP buffer at a flow rate of 5 μL min^{-1}). Immobilization of M200-AHA on Fc3 resulted in 6717 RU for chip1 and 4349 RU for chip 2.

Uniform orientation by click chemistry (Fc4): 50 μg mL^{-1} OmpA-M200-AHA in 10 mM sodium acetate, pH 4.0 was immobilized (120 μL at a flow rate of 5 μL min^{-1}) on the BCN functionalized surface. After VHH coupling, the remaining active free cyclooctynes were blocked with 35 μL 2-azidoethanol (0.1 mg mL^{-1} in HBS-EP buffer at a flow rate of 5 μL min^{-1}). Immobilization of OmpA-M200-AHA on Fc4 resulted in 4378 RU for chip 1 and 3419 RU for chip 2.

The BIAcore 3000 SPR machine was operated at a constant temperature of 25 °C and a flow of 10 μL min^{-1}. 50 μL analyte preparations in HBS-EP buffer, each of different analyte concentration, were injected over the four serially connected flow channels. Regeneration of the sensor surface was achieved with 5 μL of a 10 mM hydrogen chloride solution (HCl). Data points were measured 30 s after injection end. All sensorgrams were referenced by subtracting the signal from the reference flow channel (Fc1) and were evaluated using the BIAevaluation software.

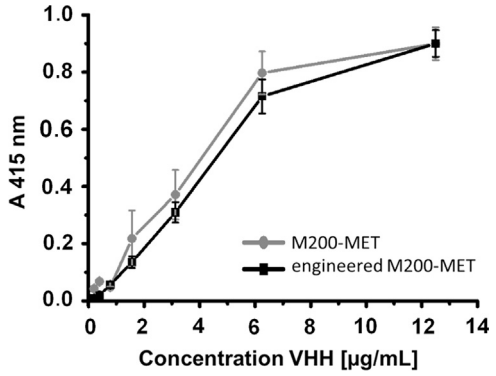

Fig. 3. Binding of engineered VHH antibody fragments to analyte investigated by ELISA. Different concentrations of VHH M200-MET and engineered M200-MET bind to surface coated analyte peptide PAT49 (for more detail see Text). Measurements were performed in duplicates, expressed as means ± SD.

2.6. Electron-spray ionization time-of-flight (ESI-ToF) measurements

VHH constructs were analyzed by ESI-ToF on a JEOL AccuToF. VHH (1 mg mL^{-1}) in 100 mM ammonium acetate was injected through an Agilent system run on MilliQ/0.1% formic acid. Deconvoluted spectra could be obtained using Mag Tran software. Calculated masses included the loss of two protons due to disulphide bond formation.

3. Results and discussion

3.1. Engineering of azide-containing llama heavy-chain antibodies domains (VHH)

To study oriented antibodies on alkyne-exposing surfaces, a VHH molecule with only a single accessible azide group was designed and

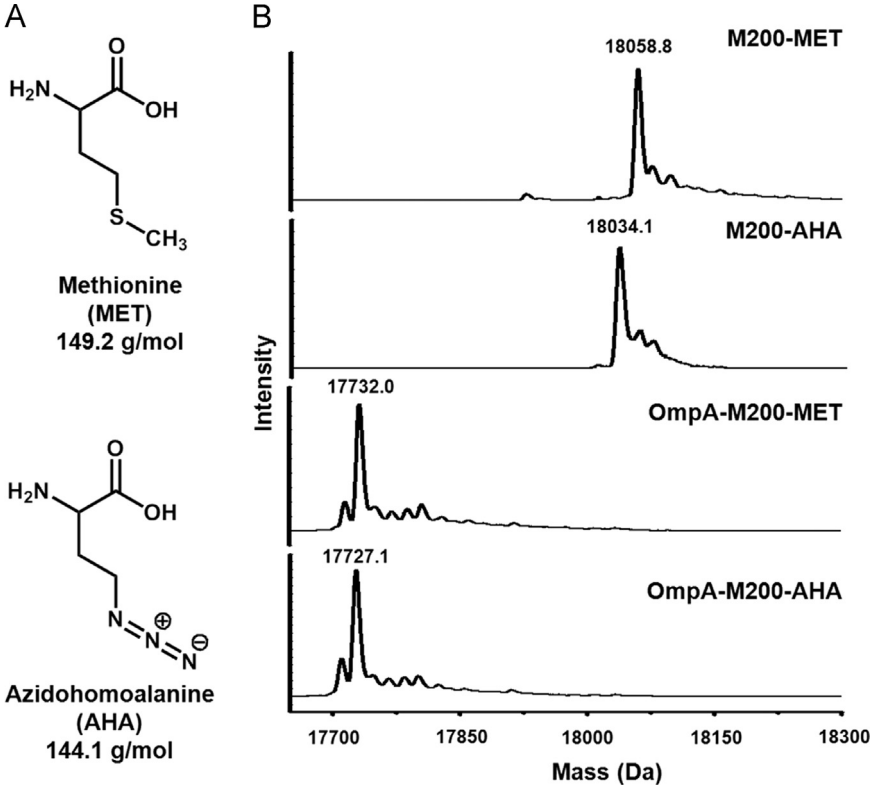

Fig. 4. Azidohomoalanine incorporation in VHH. (A) Natural amino acid methionine (MET) shows similar structure than its non-natural analog azidohomoalanine (AHA) (B) Electronspray ionization time-of-flight (ESI-ToF) mass spectra of M200 and OmpA-M200. Upon deconvolution, peaks corresponding to the calculated masses (18,058.1 Da for M200-MET, 18,033.1 Da for M200-AHA, 17,732.5 Da for OmpA-M200-MET and 17,727.5 Da for OmpA-M200-AHA) were detected.

compared to a VHH with five accessible azides. VHH M200, which recognizes the virus FMDV (Harmsen et al., 2007), normally contains five methionine positions, and can thus be immobilized in five orientations upon AHA introduction. M200 was mutated to remove those methionines, and to introduce a single, C-terminal methionine group (OmpA-M200, Fig. 2). The C-terminus is one of the exposed parts of the VHH protein, and located opposite of the analyte binding site. Immobilization via this part of the protein would thus orient the VHH to expose its analyte binding region to the solvent (Fig. 1B). To study the influence of replacing the internal methionine residues on binding affinity towards the analyte, VHHs were examined by enzyme linked immunosorbent assay (ELISA). The original VHH M200, containing five methionine residues, showed similar ELISA responses as the engineered M200 (with altered mehionines [M83, M88 and M153] and a methionine introduced at the C-terminus, Fig. 2) (Fig. 3). This indicates that in this VHH, replacement of the internal methionine residues does not interfere with analyte binding. To introduce the azide functionality in the VHHs, proteins were expressed in a methionine auxotrophic *E. coli* strain supplied with AHA in the medium. The efficient incorporation of AHA was confirmed in purified proteins by ESI-ToF mass spectroscopy.

3.2. Azide incorporation into VHH

MET differs by 5 Da in molecular mass to AHA (Fig. 4). In Fig. 4B, mass spectra of the M200-MET protein, the OmpA-M200-MET protein (both produced with MET) and the M200-AHA and OmpA-M200-AHA (both produced with AHA) are shown. The mass of M200-MET (18,058.8 Da) corresponds to a full-length M200 protein, including an N-terminal MET (Fig. 4B). The mass of M200-AHA (18,034.1 Da) is 24.7 Da lower, indicating replacements of all five MET residues by AHA. For the OmpA-M200-MET protein, the observed mass (17,732.0 Da) corresponds to a protein starting from the glutamine immediately after the OmpA cleavage site (Fig. 2B and Fig. 4B).

The mass of OmpA-M200-AHA protein (17,727.1 Da) is 4.9 Da lower than the mass of the OmpA-M200-MET protein, indicating replacement of a single MET residue by AHA. Neither mutation, nor AHA incorporation had an effect on the binding affinity of the VHH towards the analyte as shown by ELISA experiments (Fig. 5).

3.3. Accessibility of incorporated azide group

To investigate the accessibility of incorporated azide groups in the AHA-functionalized proteins, VHH proteins were reacted with alkyne-labelled polyethylene glycol (PEG). Three reactive PEG ligands were tested. The alkyne-PEG_{5000} was reacted to the protein using the CuAAC reaction. PEG_{2000} coupled to dibenzocyclooctyne (DIBO) and PEG_{5000} coupled to bicy-clo[6.1.0]non-4-yn-9-ol (BCN) were reacted to the protein by a SPAAC reaction. Increases in molecular weight of the proteins by click reactions to the PEG moieties were examined by observing mobility shifts of VHH on SDS-PAGE (Fig. 6). Protein M200-AHA, bearing five AHA residues, showed an array of mobility shift bands after reaction to alkyne-PEG_{5000} via CuAAC (Fig. 6A). This indicates that multiple azide groups in M200-AHA are available for the click reaction. For protein OmpA-M200-AHA, all three click reactions showed mobility shifts corresponding to the coupling of a single PEG unit (Fig. 6A–C).

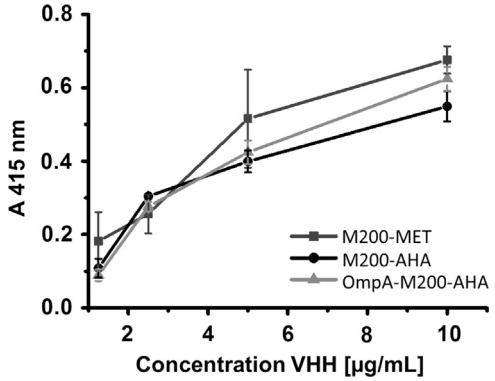

Fig. 5. Binding of azidohomoalanine functionalized VHH antibody fragments to analyte investigated by ELISA. Different concentrations of VHH M200 and OmpA-M200 bind to surface coated analyte peptide PAT49. Measurements were performed in duplicates, expressed as means ± SD.

3.4. Effect of oriented VHH in SPR biosensor

Based on this knowledge, an SPR biosensor surface was functionalized with BCN. Both azide-functionalized VHHs – M200-AHA and OmpA-M200-AHA – were immobilized in separate SPR channels via the SPAAC reaction. M200-AHA will couple to the surface by either one of the five exposed azide groups, thus allowing five different orientations (Fig. 1C). In contrast, OmpA-M200-AHA contains only one azide group at the C-terminus and will attach in a uniform direction on the surface (Fig. 1B). For comparison to conventional random immobilization methods, an SPR channel that was functionalized using NHS chemistry was included in the analysis. Two analytes were tested: FMDV viral particles (60 recognition sites), and peptide PAT49, which is the known epitope towards the antibody, with one recognition site.

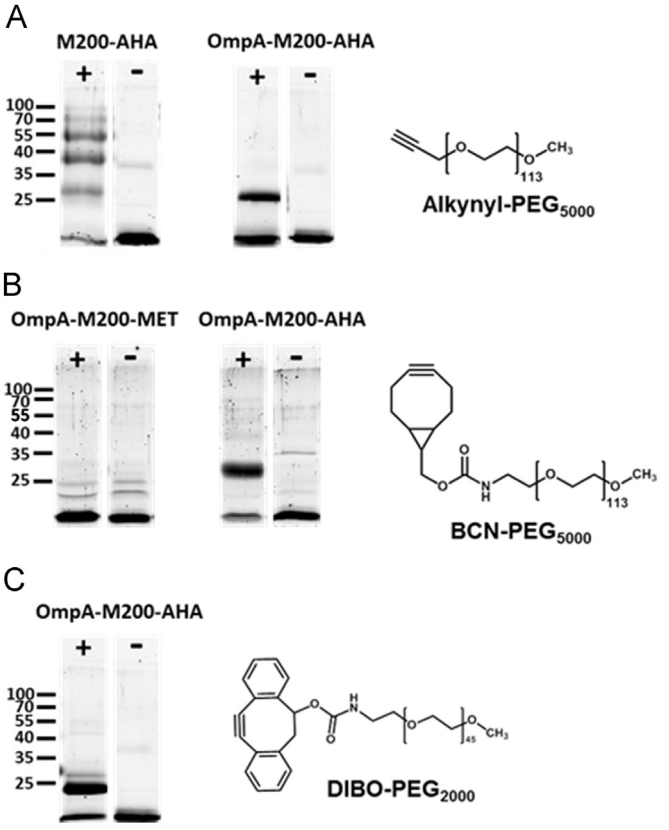

Fig. 6. PEG-reacted VHHs size separated by sodium dodecyl sulfate polyacrylamide gel electrophoresis. (A) M200-AHA and OmpA-M200-AHA reacted with alkynl-PEG_{5000} via CuAAC (B) OmpA-M200-MET and OmpA-M200-AHA reacted with BCN-PEG_{5000} via SPAAC. (C) OmpA-M200-AHA reacted with DIBO-PEG_{2000} via SPAAC. Plus (+) indicates presence of PEG-compound, minus (−) absence. Indicated are the positions of relevant size markers in kDa.

Concentration ranges of both analytes were analyzed to investigate the sensitivity of the sensor surfaces. To our surprise, the uniformly oriented OmpA-M200 showed an 800-fold higher sensitivity for peptide PAT49 than the randomly oriented M200: the threshold value of 10 RU was reached at 0.07 μg mL^{-1} for OmpA-M200, and at 55.4 μg mL^{-1} for M200 (Fig. 7). This orientation effect of almost three orders of magnitude is, as far as we know, by far the largest orientation effect observed up to now for any antibody-mediated biosensing event. Orientation effects typically range from 1 to 10 (Yuan et al., 2011; Vashist et al., 2011; Huy et al., 2011; Balevicius et al., 2011) with only a handful reports that indicate significantly larger ones (Park et al., 2011a, 2011b; Yoo et al., 2011).

For FMDV, the signals were much stronger, and the orientation effect was less pronounced. Still ~10-fold higher sensitivity was observed in the oriented channel (Fig. 7). Previously we studied the effect of analyte properties, such as the number of recognition sites, the molecular weight and the affinity, on the biosensor response, using streptavidin-biotin and NHS chemistry (Trilling et al., 2013a). In that study it was already observed that the signal response of peptide PAT49 benefits (14-fold) from orientation, while detection of FMDV only marginally (2-fold) improved. These differences appeared to depend on the higher affinity of FMDV for the M200 antibody: with a lower affinity, the orientation effects increased. In the current work we measure the threshold of analyte detection, which is the parameter of interest for pathogen diagnostics. It is not fully clear why the current orientation enhancement is even bigger, and more experimentation is required for a further development of the hypothesis, but the sheer magnitude of this effect holds great promise for diagnostics.

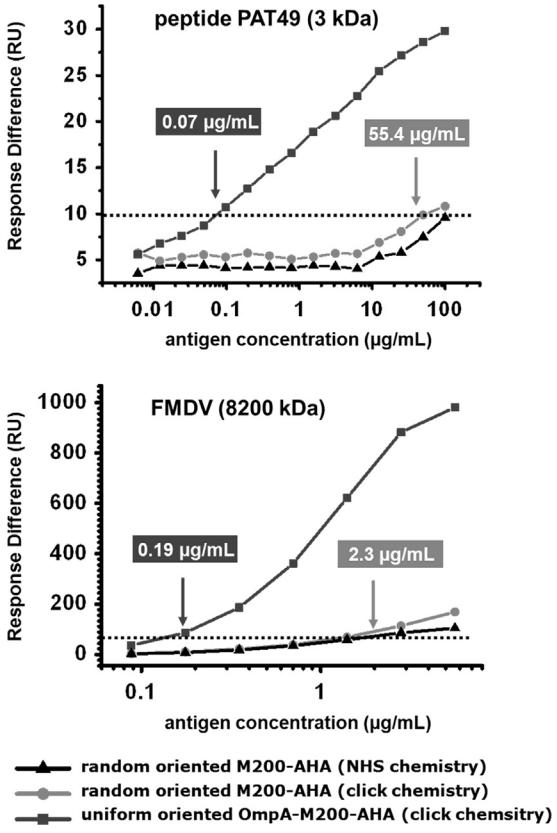

Fig. 7. Surface plasmon resonance analysis of M200-AHA and OmpA-M200-AHA functionalized sensors. A dilution series of peptide PAT49 (100 μg mL^{-1}–0.006 μg mL^{-1}) and FMDV (5.6 μg mL^{-1}–0.08 μg mL^{-1}) was simultaneously analyzed on randomly oriented (M200-AHA click chemistry [circles] and M200-AHA NHS chemistry [triangles]) and uniformly oriented (OmpA-M200-AHA click chemistry [squares]) channels.

As a negative control bovine serum albumin was tested, but did not produce a change in the RU (ESI, Fig. S1). To investigate the stability of VHHs attached to the surface via the various immobilization strategies, repeated cycles of peptide PAT49 and FMDV injection and regeneration with 5 μL 10 mM HCl were performed. VHH immobilized by click chemistry show an average signal loss of 0.23% after each cycle, whereas VHHs immobilized by NHS chemistry show an average signal loss of 0.26% after each cycle (ESI: Table S2). In other words: the azide-alkyne click reaction provides a covalent link that is at least as good as NHS-induced amide bond formation.

4. Conclusion

In summary, previously the effect of orientation of antibodies has been studied using different immobilization strategies, which may complicate comparisons (Vashist et al., 2011; Huy et al., 2011). The current study was performed using identical (SPAAC) chemistry for uniform and random immobilization, before comparing their sensing properties. Under these circumstances, orienting antibodies on sensor surfaces by click chemistry leads to strongly improved sensitivity of biosensors, up to a factor 800. Such orientation effects thus greatly enhance the potential of diagnostics, which is crucial for the early detection of diseases that is needed to contain spreading of aggressive viruses such as FMDV. Finally, further improvements may be anticipated by combining orienting proteins with tuning surfaces at the nanoscale, such as via polymer brushes or monolayers, as this will allow to create more intelligent materials (Nguyen et al., 2011).

Acknowledgements

This work was funded by the European Union through the Marie Curie Integrated Training Network project Hierarchy (contract: PITN-2007-215851). Sponsors had no influence in study design; collection, analysis, and interpretation of data; in the writing of the report; and in the decision to submit the paper for publication. The help and suggestions made by Angelique Wammes, Michiel Harmsen, Vincent Ruigrok and Willem Haasnoot are kindly acknowledged. The authors also like to thank Marjoke Debets for supply of DIBO-PEG$_{2000}$.

Appendix A. Supporting information

Supplementary data associated with this article can be found in the online version at http://dx.doi.org/10.1016/j.bios.2014.04.017.

References

Balevicius, Z., Ramanaviciene, A., Baleviciute, I., Makara-viciute, A., Mikoliunaite, L., Ramanavicius, A., 2011. Sens. Actuators, B 160, 555–562.
Bereli, N., Şener, G., Yavuz, H., Denizli, A., 2011. Mater. Sci. Eng., C 31, 1078–1083.
Bradford, M.M., 1976. Anal. Biochem. 72, 248–254.
Chen, H., Huang, J., Lee, J., Hwang, S., Koh, K., 2010. Sens. Actuators, B B147, 548–553.
Conroy, P.J., Hearty, S., Leonard, P., O'Kennedy, R.J., 2009. Semin. Cell Dev. Biol. 20, 10–26.
Debets, M.F., van Berkel, S.S., Dommerholt, J., Dirks, A.J., Rutjes, F.P.J.T., van Delft, F.L., 2011. Acc. Chem. Res. 44, 805–815.
Deffar, K., Shi, H., Li, L., Wang, X., Zhu, X., 2009. Afr. J. Biotechnol. 8, 2645–2652.
Deiters, A., Cropp, T.A., Summerer, D., Mukherji, M., Schultz, P.G., 2004. Bioorg. Med. Chem. Lett. 14, 5743–5745.
Hamers-Casterman, T.A.C., Muyldermans, S., Robinson, G., Hammers, C., Bajyana Songa, E., Bendahman, N., Hammers, R., 1993. Nature 363, 446–448.
Harmsen, M.M., van Solt, C.B., Fijten, H.P.D., van Keulen, L., Rosalia, R.A., Weerdmeester, K., Cornelissen, A.H.M., De Bruin, M.G.M., Eblé, P.L., Dekker, A., 2007. Vet. Microbiol. 120, 193–206.

Hong, V., Steinmetz, N.F., Manchester, M., Finn, M.G., 2010. Bioconjugate Chem. 21, 1912–1916.
Huy, T.Q., Hanh, N.T.H., van Chung, P., Anh, D.D., Nga, P.T., Tuan, M.A., 2011. Appl. Surf. Sci. 257, 7090–7095.
Jewett, J.C., Bertozzi, C.R., 2010. Chem. Soc. Rev. 39, 1272–1279.
Kiick, K.L., Saxon, E., Tirrell, D.A., Bertozzi, C.R., 2002. Proc. Nat. Acad. Sci. 99, 19–24.
Kolb, H.C., Finn, M.G., Sharpless, K.P., 2001. Angew. Chem. Int. Ed. 40, 2004–2021.
Nguyen, A.T., Baggerman, J., Paulusse, J.M.J., Zuilhof, H., van Rijn, C.J.M., 2011. Langmuir 28, 604–610.
Park, J.W., Cho, I.H., Moon, D.W., Paek, S.H., Lee, T.G., 2011a. Surf. Interface Anal. 43, 285–289.
Park, M., Jose, J., Pyun, J.C., 2011b. Sens. Actuators, B. 154, 82–88.
Saerens, D., Frederix, F., Reekmans, G., Conrath, K., Jans, K., Brys, L., Huang, L., Bosmans, E., Maes, G., Borghs, G., Muyldermans, S., 2005. Anal. Chem. 77, 7547–7555.
Schoffelen, S., Lambermon, M.H.L., van Eldijk, M.B., van Hest, J.C.M., 2008. Bioconjugate Chem. 19, 1127–1131.
Song, H.Y., Zhou, X., Hobley, J., Su, X., 2011. Langmuir 28, 997–1004.
Schoffelen, S., Schobers, L., Venselaar, H., Vriend, G., v Hest, J.C.M., 2010. Green Polymer Chemistry: Biocatalysis and Biomaterials. 1043. American Chemical Society, pp. 125–139.
Trilling, A.K., de Ronde, H., Noteboom, L., van Houwelingen, A., Roelse, M., Srivastava, S.K., Haasnoot, W., Jongsma, M.A., Kolk, A., Zuilhof, H., Beekwilder, J., 2011. PLoS One 6, e26754.
Trilling, A.K., Harmsen, M.M., Ruigrok, V.J.B., Zuilhof, H., Beekwilder, J., 2013a. Biosens. Bioelectron. 40, 219–226.
Trilling, A.K., Beekwilder, J., Zuilhof, H., 2013b. Analyst 138, 1619–1627.
Vashist, S.K., Dixit, C.K., MacCraith, B.D., O'Kennedy, R., 2011. Analyst 136, 4431–4436.
van Houwelingen, A.M.M.L., de Saeger, T., Rusanova, T., Waalwijk, C., Beekwilder, M. J., 2008. World Mycotoxin J. 1, 407–417.
Yoshimoto, K., Nishio, M., Sugasawa, H., Nagasaki, Y., 2010. J. Am. Chem. Soc. 132, 7982–7989.
Yoo, G., Park, M., Lee, E.H., Jose, J., Pyun, J.C., 2011. Anal. Chim. Acta 707, 142–147.
Yuan, Y., Yin, M., Qian, J., Liu, C., 2011. Soft Matters 7, 7207–7216.
Zeng, X., Shen, Z., Mernaugh, R., 2012. Anal. Bioanal. Chem. 402, 3027–3038.